[Research Paper] 대한금속 · 재료학회지 (*Korean J. Met. Mater.*), Vol. 62, No. 4 (2024) pp.299-305
DOI: 10.3365/KJMM.2024.62.4.299

Improvement in the Hydrogen-Storage Properties of Mg_2Ni by Adding $LiBH_4$

Young Jun Kwak[1,2], Myoung Youp Song[1,2,*], and Ki-Tae Lee[1,2,3]

[1]*Division of Advanced Materials Engineering, Jeonbuk National University, 567 Baekje-daero Deokjin-gu Jeonju, 54896, Republic of Korea*
[2]*Hydrogen & Fuel Cell Research Center, Engineering Research Institute, Jeonbuk National University, 567 Baekje-daero Deokjin-gu Jeonju, 54896, Republic of Korea*
[3]*Department of Energy Storage/Conversion Engineering of Graduate School (BK21 FOUR), Jeonbuk National University, 567 Baekje-daero Deokjin-gu Jeonju, 54896, Republic of Korea*

Abstract: To improve the hydrogen-storage properties of Mg_2Ni, $LiBH_4$ was added by milling in hydrogen atmosphere (reactive mechanical milling, RMM). Mg_2Ni-10$LiBH_4$ was prepared with a composition of 90 wt% Mg_2Ni + 10 wt% $LiBH_4$. The quantity of released hydrogen (H_r) versus temperature T curve for Mg_2Ni-10$LiBH_4$ was obtained by heating at a rate of 4~5 K in 1.0 bar hydrogen. The hydrogen-storage properties of the sample were investigated. The phases formed were examined from the x-ray diffraction (XRD) patterns of the samples after RMM, and after hydrogen-absorption and release cycling. The XRD pattern of Mg_2Ni-10$LiBH_4$ showed that this sample contained Mg_2Ni, Mg_2NiH_4, o-$LiBH_4$, h-$LiBH_4$, Ni, and MgH_2. The dH_r/dT versus T curve exhibited three peaks at 325 K, 563 K, and 600 K, respectively. The peak at 325 K is for the hydrogen release from o-$LiBH_4$ and h-$LiBH_4$. The peak at 563 K is for the hydrogen release from Mg_2NiH_4 and the peak at 600 K is for the hydrogen release from Mg_2NiH_4 and MgH_2. The RMM of Mg_2Ni with added $LiBH_4$ creates defects and cracks. RMM facilitates nucleation, increases reactivity, and shortens the diffusion distances of hydrogen atoms. Expansion and contraction of lattices due to cycling has effects similar to, but weaker than, the effects of RMM.

(Received 23 November, 2023; Accepted 6 January, 2024)

Keywords: hydrogen-storage properties, Mg_2Ni, $LiBH_4$, XRD patterns, hydrogen absorption and release curves

1. INTRODUCTION

To use hydrogen as an energy carrier, effective techniques for hydrogen generation and storage must be developed. Metal hydrides have been studied for hydrogen storage in solid state by many researchers [1-9]. One of other methods to store hydrogen is using the adsorption of hydrogen by zeolites [10]. A method to store hydrogen in gas state under high pressure is using a tank, for which employing the composites of carbon nanotubes (CNTs) dispersed in epoxy resin was studied [11].

Reilly and Wiswall [12] first investigated the hydrogen storage properties of Mg_2NiH_4. They reported that Mg_2Ni reacted readily with hydrogen in 20 bar at 598 K, and Mg_2Ni reacted reversibly with hydrogen according to the following reaction:

$$Mg_2Ni + H_2 \Leftrightarrow Mg_2NiH_4. \quad (1)$$

The equilibrium plateau pressure is 1 bar at 527 K for the Mg_2Ni-H system [13] and at 557 K for the Mg-H system [14]. Mg_2NiH_4 thus releases hydrogen at slightly lower temperatures than MgH_2. Reilly and Wiswall [12] reported that the Mg_2Ni produced by conventional ingot metallurgy required several cycles at 573 K for activation. To use Mg_2NiH_4 as a solid-state hydrogen-storage material, the relatively high temperature of hydrogen-absorption and release should be lowered, the rather slow reaction kinetics should be improved, and the quite difficult activation should be solved.

It was reported that lithium borohydride, $LiBH_4$, has high gravimetric and volumetric hydrogen capacities (18.5 wt% and 121 kg H_2 m^{-3}). The melting point of $LiBH_4$ is 541 K and

- Young Jun Kwak: 연구원, Myoung Youp Song: 교수, Ki-Tae Lee: 교수
**Corresponding Author:* Myoung Youp Song
[Tel: +82-10-3260-2379, E-mail: songmy@jbnu.ac.kr]

the boiling point (at which it decomposes) is 653 K [15]. Züttel et al. [16] reported the thermal hydrogen-release process of $LiBH_4$. They found that the low temperature release from the orthorhombic phase liberates only a small amount (0.3 wt%) of hydrogen and the high temperature phase liberates up to 13.5 wt% of hydrogen (3 mol H per $LiBH_4$). 4.5 wt% of the hydrogen remains as LiH in the decomposition product. Ding et al. [17] reported that $LiBH_4$ is now the leading candidate for onboard hydrogen storage, but the reversible capacity of hydrogen storage of $LiBH_4$ should be increased. Vajo et al. [18,19] reported that $LiBH_4$ has a high hydrogen-storage capacity, but an equilibrium plateau pressure of 1 bar for $LiBH_4$ would require a temperature of over 673 K, due to its high thermal stability.

In previously reported works to develop hydrogen-storage materials, $LiBH_4$ has been mixed with MgH_2 [18-28], $Mg_{11}CeNi$ [29], and Mg_2NiH_4 [30,31], but not Mg_2Ni. Ding et al. [17] reported that high-energy ball milling with in-situ aerosol spraying may improve the reaction kinetics in thermodynamically favorable systems such as $LiBH_4$+ MgH_2 mixture and provide the thermodynamic driving force needed to lower the hydrogen release temperature [17]. Vajo et al. [18,19] tried to decrease the decomposition temperature to about 498 K at an equilibrium plateau pressure of 1 bar by adding MgH_2, which lowered the thermal stability of $LiBH_4$. When MgH_2 was added to $LiBH_4$, MgB_2 was formed. The formation of MgB_2 upon hydrogen release destabilized $LiBH_4$. D.M. Liu et al. [29] used a hydrogenated $Mg_{11}CeNi$ alloy as a destabilizer of $LiBH_4$. They reported that thermal dehydrogenation of the $17LiBH_4$ + $2.5Mg_{11}CeNi$ hydride begins at around 553 K with about 4.0 wt% of hydrogen released from MgH_2 and Mg_2NiH_4, and then $LiBH_4$ co-destabilized by Mg_2Ni, CeH_2 and Mg decomposes in the temperature range 623 – 698 K. These two-step reactions were partially reversible and about 4.9 wt% of hydrogen could be reloaded at 673 K under an initial hydrogen pressure of 90 bar. Vajo et al. [30] added Mg_2NiH_4 to $LiBH_4$ and they reported that the $LiBH_4$/Mg_2NiH_4 system was a reversible mixed complex hydride system and $LiBH_4$ and Mg_2NiH_4 released hydrogen cooperatively, beginning at 23 K. However, they reported that the hydrogen capacity and hydrogen absorption and release kinetics do not meet requirements for practical use. Bergemann et al. [31] investigated the hydrogen sorption properties of the $2LiBH_4$ + $2.5Mg_2NiH_4$ composite system as a function of the applied temperature and hydrogen pressure. They reported that $LiBH_4$ and Mg_2NiH_4 were destabilized mutually.

In the present work, to improve the hydrogen-storage properties of Mg_2Ni, $LiBH_4$ was added to Mg_2Ni by milling in hydrogen atmosphere (reactive mechanical milling, RMM). Mg_2Ni-$10LiBH_4$ (with a composition of 90 wt% Mg_2Ni + 10 wt% $LiBH_4$) was prepared. The quantity of released hydrogen (H_r) versus temperature T curve for Mg_2Ni-$10LiBH_4$ was obtained by heating at a rate of 4~5 K in 1.0 bar hydrogen. The phases formed were examined using the x-ray diffraction (XRD) patterns of the samples after RMM and after hydrogen-absorption and release cycling. The hydrogen-storage properties of the sample were investigated.

2. EXPERIMENTAL DETAILS

As starting materials, MgH_2 (Magnesium hydride, 98%, Alfa Aesar), Ni (average particle size 2.2–3.0 um, purity 99.9 % metal basis, C typically < 0.1%, Alfa Aesar), Mg_2Ni (powder, purity: 99.5%, 150 mesh, Toshima, Japan), and $LiBH_4$ (purity >90%, Aldrich) were used.

Samples were prepared by milling in hydrogen atmosphere (reactive mechanical grinding). All materials were handled in a glove box filled with Ar gas. In a planetary ball mill (Planetary Mono Mill; Pulverisette 6, Fritsch), 8 g mixtures with planned compositions were put into a stainless steel container together with 105 hardened steel balls (total weight = 360 g), the sample to ball weight ratio being 1 : 45. The stainless steel container (volume = 250 ml) was then filled with hydrogen at 12 bar. The milling in hydrogen was carried out by repeatedly milling for 15 min and pausing for 5 min, for 24 cycles, with total milling time being 6 h. The disc revolution speed was 400 rpm. Hydrogen pressure of 12 bar was restored by refilling every 2 hours.

The quantity of released hydrogen versus temperature curve for the prepared sample was obtained by heating the sample at a heating rate of 4~5 K in 1.0 bar hydrogen, using a volumetric method in a Sieverts-type hydrogen-absorption and release apparatus, which was previously described [32]. Variations in absorbed or released hydrogen quantities with

time were also measured using a volumetric method in this apparatus. For hydrogen absorption and release measurements at a constant temperature, the hydrogen pressures were kept nearly constant. After hydrogen absorption, the hydrogen absorbed (leading to a decrease in the hydrogen pressure in the reactor) was refilled to the reactor from a standard reservoir with a known volume, the pressure regulator being opened automatically. For hydrogen release, the hydrogen released (leading to an increase in the hydrogen pressure in the reactor) was removed from the reactor to the standard reservoir, the back-pressure regulator automatically being opened. For these measurements, 0.5 g of powder samples were put into the reactor and the reactor was vacuum-pumped.

The X-ray diffraction (XRD) patterns of samples after reactive mechanical grinding and those after hydrogen absorption-release cycling were obtained with Cu Kα radiation in a Bruker D8 Advance (Karlsruhe, Germany) powder diffractometer. The Jade 6 program was used to analyze the phases in the samples from the XRD patterns.

3. RESULTS AND DISSCUSSION

Fig. 1 shows the XRD patterns of Mg_2Ni-10$LiBH_4$ after reactive mechanical milling (RMM). The XRD pattern of Mg_2Ni-10$LiBH_4$ after RMM shows the materials were in an amorphous state with a wide peak (between 33° and 50° of diffraction angles) and high background. In amorphous materials the atoms of are located irregularly, unlike the atoms in crystalline materials. The XRD pattern of Mg_2Ni-10$LiBH_4$ shows that this sample contains Mg_2Ni, Mg_2NiH_4, o-$LiBH_4$, h-$LiBH_4$, Ni, and MgH_2. It appears that there are peaks of the Ni_4B_3 phase, but we are not certain of its presence. Karimi et al. [21] reported that orthorhombic $LiBH_4$ (o-$LiBH_4$) is transformed to hexagonal $LiBH_4$ (h-$LiBH_4$) at temperatures higher than 388 K. We think that Mg and Ni were contained in the purchased Mg_2Ni and Mg formed MgH_2 during RMM. During reactive mechanical milling, the following reaction occurs mainly:

$$2Mg_2Ni + 2o\text{-}LiBH_4 + Mg + Ni + 3H_2 \rightarrow Mg_2Ni + Mg_2NiH_4 + o\text{-}LiBH_4 + h\text{-}LiBH_4 + MgH_2 + Ni. \quad (1)$$

The quantity of released hydrogen, H_r, is defined using the sample weight as a standard.

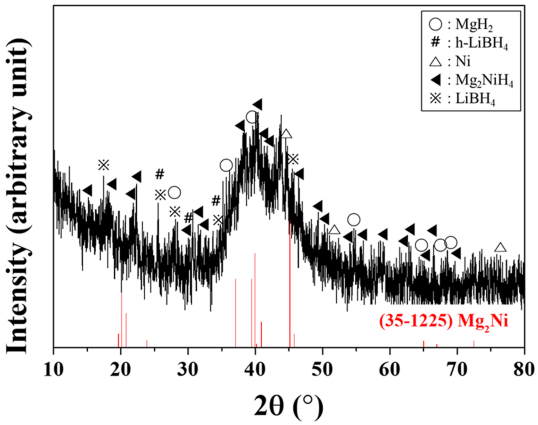

Fig. 1. XRD pattern of Mg_2Ni-10$LiBH_4$ after reactive mechanical milling.

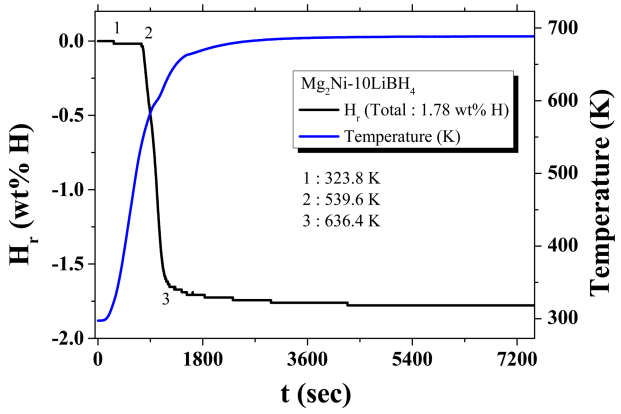

Fig. 2. Quantity of released hydrogen (H_r) versus temperature T curve for Mg_2Ni-10$LiBH_4$. The sample was heated at a heating rate of 4~5 K in 1.0 bar hydrogen.

The quantity of released hydrogen (H_r) versus temperature T curve for Mg_2Ni-10$LiBH_4$ is shown in Fig. 2. The sample was heated at a heating rate of 4~5 K in 1.0 bar hydrogen. In the beginning, the prepared sample releases hydrogen very rapidly for about 8.8 min, the total released hydrogen being 1.78 wt%. The sample begins to release hydrogen at 323.8 K, begins to release hydrogen very rapidly at 539.6 K, and releases very slowly from 636.4 K. It is believed that o-$LiBH_4$ and h-$LiBH_4$ begin to release hydrogen at 323.8 K and Mg_2NiH_4 and MgH_2 begin to release hydrogen at 539.6 K.

Fig. 3 shows the H_r versus T and dH_r/dT versus T curves for Mg_2Ni-10$LiBH_4$. The sample was heated at a heating rate of 4~5 K in 1.0 bar hydrogen. The dH_r/dT versus T curve exhibits three peaks at 325 K, 563 K, and 600 K,

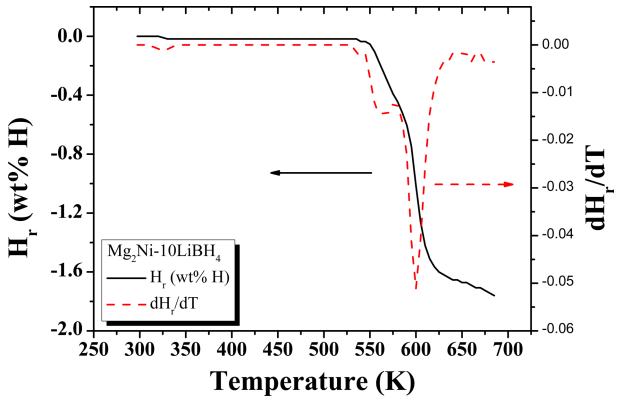

Fig. 3. H_r versus T and dH_r/dT versus T curves for Mg_2Ni-$10LiBH_4$. The sample was heated at a heating rate of 4~5 K in 1.0 bar hydrogen.

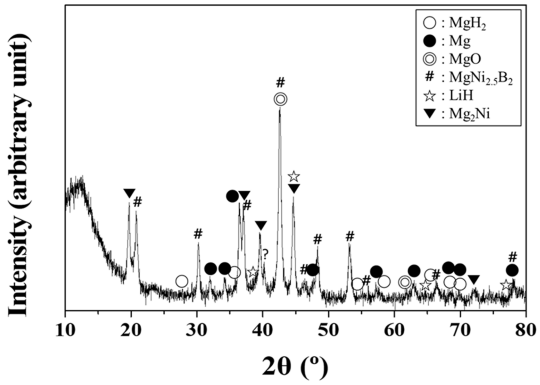

Fig. 4. XRD pattern of Mg_2Ni-$10LiBH_4$ dehydrided after four hydrogen-absorption and release cycles.

respectively. The peak at 325 K is for the hydrogen release from o-$LiBH_4$ and h-$LiBH_4$. The peak at 563 K is for the hydrogen release from Mg_2NiH_4 and the peak at 600 K is for the hydrogen release from Mg_2NiH_4 and MgH_2.

The XRD patterns of dehydrided Mg_2Ni-$10LiBH_4$ after four hydrogen absorption-release cycles are shown in Fig. 4. The dehydrided Mg_2Ni-$10LiBH_4$ contains Mg_2Ni, $MgNi_{2.5}B_2$, Mg, MgH_2, LiH, and MgO. MgO is believed to be formed during treatment in air to produce the XRD pattern. Ni, which exists in the sample after RMM, was not observed. During heating to 593 K, the following reaction occurs:

$$5Mg_2Ni + 2Mg_2NiH_4 + 2o\text{-}LiBH_4 + 2h\text{-}LiBH_4 + 2MgH_2 \rightarrow 2Mg_2Ni + 2MgNi_{2.5}B_2 + 9Mg + MgH_2 + 4LiH + 11H_2. \quad (2)$$

Mg_2Ni and Ni form $MgNi_{2.5}B_2$ by reacting with B from $LiBH_4$, leading to the separation of Mg to form Mg_2Ni. It is

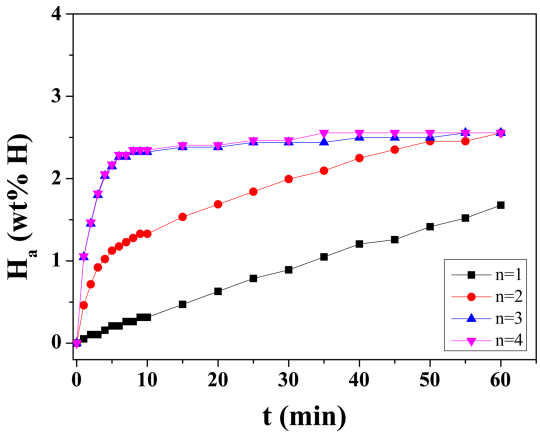

Fig. 5. Variation in the curve of absorbed hydrogen quantity (H_a) versus time t with the number of cycles, n, at 593 K in 12 bar hydrogen for Mg_2Ni-$10LiBH_4$.

believed that Ni, which exists in the sample after RMM, is not observed in the XRD pattern of dehydrided Mg_2Ni-$10LiBH_4$ after four hydrogen-absorption and release cycles (Fig. 4) because Ni was used to form $MgNi_{2.5}B_2$. The formation of $MgNi_{2.5}B_2$, which cannot absorb and release hydrogen during the hydrogen absorption and release reactions, respectively, decreases the content of Mg_2Ni even though it produces Mg. The formation of $MgNi_{2.5}B_2$ thus leads to a decrease in the hydrogen-storage capacity of the Mg_2Ni-$10LiBH_4$ sample. The Mg atoms in either Mg_2Ni or Mg absorb the same number of hydrogen atoms because they form Mg_2NiH_4 and MgH_2, respectively. During the hydrogen-absorption and release reactions, the following reactions occur:

$$Mg_2Ni + MgNi_{2.5}B_2 + Mg + MgH_2 + LiH + 3H_2 \Leftrightarrow Mg_2NiH_4 + MgNi_{2.5}B_2 + 2MgH_2 + LiH. \quad (3)$$

Bergemann et al. [30] analyzed the powder x-ray diffractions of $2LiBH_4 + 2.5Mg_2NiH_4$ composites dehydrogenated in hydrogen pressures of 1, 5, and 50 bar. They reported that all the samples contained $MgNi_{2.5}B_2$ and $2MgH_2$. Mg was found in the samples dehydrogenated in hydrogen pressures of 1 and 5 bar.

The initial hydrogen-absorption rate is defined as the hydrogen-absorption rate from beginning to 1 min. The effective hydrogen-storage capacity is defined as the quantity of hydrogen absorbed in 60 min.

Fig. 5 shows the variation in the curve of absorbed

hydrogen quantity (H_a) versus time t with the number of cycles, n, at 593 K in 12 bar hydrogen for Mg_2Ni-10$LiBH_4$. At n = 1, Mg_2Ni-10$LiBH_4$ absorbs 0.21 wt% H for 5 min, 0.89 wt% H for 30 min, and 1.68 wt% H for 60 min. The initial hydrogen-absorption rate increases from n = 1 to n = 3 quite rapidly. From n = 3 to n = 4, the initial hydrogen-absorption rate increases a little bit. The effective hydrogen-storage capacity increases a lot from n = 1 to n = 2 and remains almost the same from n = 2 to n = 4. The activation is accomplished at n = 3. The initial hydrogen-absorption rates are 0.05, 1.05, and 1.06 wt% H/min at n = 1, n = 3, n = 4, respectively. The effective hydrogen-storage capacity is 2.56 wt% at n = 3. Mg_2Ni-10$LiBH_4$ absorbs 2.15 wt% H for 5 min, 2.44 wt% H for 30 min, and 2.56 wt% H for 60 min at n =3. At n = 1, H_a increases almost linearly as the reaction time elapses. At n = 2 ~ 4, the H_a versus t curves exhibits a quite high initial hydrogen-absorption rate region and then a lower hydrogen-absorption rate region. It is believed that hydrogen is absorbed to Mg_2Ni in the former and to Mg in the latter. Equation (3) shows that Mg_2Ni and Mg participate the hydrogen-absorption and release reactions. Expansion due to hydrogen absorption and contraction due to hydrogen release create defects on the surfaces of particles and inside the particles. The defects and formed phases act as centers of stress and thus cracks can be initiated from the defects and formed phases. Propagation of the initial cracks makes the particles finer. The defects and formed phases also act as active sites for nucleation. Crack formation produces clean surfaces, leading to an increase in the reactivity of the particles. Reducing the particle size shortens the diffusion distances for hydrogen atoms. D.M. Liu et al. [29] reported that the 17$LiBH_4$ + 2.5$Mg_{11}CeNi$ hydride absorbed about 4.9 wt% of hydrogen at 673 K under an initial hydrogen pressure of 90 bar, which is larger than the effective hydrogen-storage capacity of Mg_2Ni-10$LiBH_4$ for this work. It is believed that more hydrogen was absorbed by the 17$LiBH_4$ + 2.5$Mg_{11}CeNi$ sample than Mg_2Ni-10$LiBH_4$ because $LiBH_4$ had higher content and higher temperature and hydrogen pressure for hydrogen absorption.

The variation in the curve of released hydrogen quantity (H_r) versus t with the number of cycles, n, at 593 K in 1.0 bar hydrogen for Mg_2Ni-10$LiBH_4$.is shown in Fig. 6. At n = 1, Mg_2Ni-10$LiBH_4$ releases 0.55 wt% H for 5 min, 1.49 wt% H for 30 min, and 1.67 wt% H for 60 min. The initial hydrogen-release rate is defined as the hydrogen-release rate from beginning to 1 min. The initial hydrogen-release rate increases from n = 1 to n = 2 quite rapidly. From n = 2 to n = 4, the initial hydrogen-release rate remains almost the same. The released hydrogen quantity for 60 min increases rapidly from n = 1 to n = 2 and remains unchanged from n = 2 to n = 4. The initial hydrogen-release rates are 0.12, 0.25, and 0.23 wt% H/min at n = 1, n = 2, n = 3, respectively. Mg_2Ni-10$LiBH_4$ releases 1.08 wt% H for 5 min, 2.48 wt% H for 30 min, and 2.56 wt% H for 60 min at n = 3. At n = 1 ~ 4, the H_r versus t curves exhibit a quite high initial hydrogen-release rate region and then a lower hydrogen-release rate region. It is believed that hydrogen is released from Mg_2NiH_4 in the former and from MgH_2 in the latter.

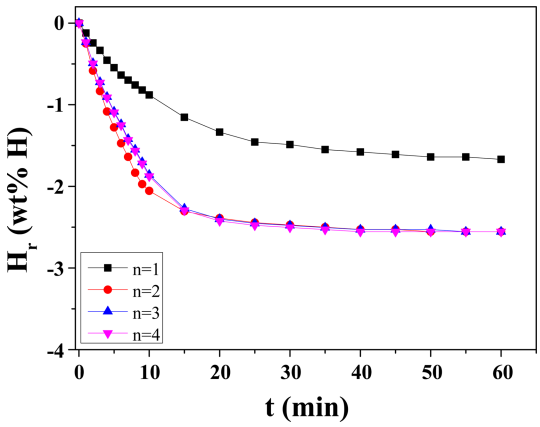

Fig. 6. Variation in the curve of released hydrogen quantity (H_r) versus t with the number of cycles, n, at 593 K in 1.0 bar hydrogen for Mg_2Ni-10$LiBH_4$.

Reactive mechanical milling creates defects on the surfaces of particles and inside the particles. The defects, added phases (o-$LiBH_4$), and phases formed during RMM (Mg_2NiH_4, h-$LiBH_4$, MgH_2) initiate cracks because the defects and formed phases act as centers of stress. Propagation of the initial cracks decreases particle size. The defects, added phases, and formed phases also act as active sites for nucleation. Crack formation produces clean surfaces and increases the reactivity of particles. Reducing the particle size shortens the diffusion distances for hydrogen atoms. These increase the hydrogen-absorption and release rates. The expansion and contraction of lattices due to cycling has effects similar to, but weaker than, the effects of RMM.

4. CONCLUSIONS

The hydrogen-storage properties of Mg_2Ni were improved by adding $LiBH_4$ via milling in hydrogen atmosphere. Measurement of hydrogen release of the prepared sample in a heating rate of 4~5 K in 1.0 bar hydrogen showed that o-$LiBH_4$ and h-$LiBH_4$ began to release hydrogen at 323.8 K and Mg_2NiH_4 and MgH_2 began to release hydrogen at 539.6 K. The Mg_2Ni-10$LiBH_4$ dehydrided after hydrogen-absorption and release cycling contained Mg_2Ni, $MgNi_{2.5}B_2$, Mg, MgH_2, LiH, and MgO. During hydrogen-absorption and release cycling, Mg_2Ni and Mg participated in the reactions. The activation was accomplished at n = 3. The initial hydrogen-absorption rate was 1.05 wt% H/min and the effective hydrogen-storage capacity was 2.56 wt% at n = 3. Reactive mechanical milling (RMM) of Mg_2Ni with $LiBH_4$ added creates defects and initiates cracks. The defects and formed phases during reactive mechanical milling become centers of stress concentration, promoting the propagation of cracks. Propagation of cracks makes the particles finer. Cycling has effects similar to, but weaker than, the effects of RMM.

ACKNOWLEDGEMENT

This work was supported by the National Research Foundation of Korea (NRF) grant funded by the Korean government (MSIT) (No. 2021R1C1C2009103). This work was also supported by Korea Institute of Energy Technology Evaluation and Planning (KETEP) grant funded by the Korea government (MOTIE) (20213030040110).

REFERENCES

1. J. S. Han and K. D. Park, *Kor. J. Met. Mater.* **48**, 1123 (2010).
2. J.S. Han, M. Pezat, J.-Y. Lee, *Scr. Metall.* **20**, 951 (1986).
3. J.S. Han, M. Pezat, J.-Y. Lee, *J. Less-Common Met.* **130**, 195 (1987).
4. K. I. Kim and T. W. Hong, *Kor. J. Met. Mater.* **49**, 264 (2011).
5. J. J. Reilly and R. H. Wiswall, *Inorg. Chem.* **6**, 2220 (1967).
6. E. Akiba, K. Nomura, S. Ono, S. Suda, *Int. J. Hydrogen Energy* **7**, 787 (1982).
7. J.-L. Bobet, E. Akiba, Y. Nakamura and B. Darriet, *Int. J. Hydrogen Energy* **25**, 987 (2000).
8. J. Huot, D.B. Ravnsbæk, J. Zhang, F. Cuevas, M. Latroche, T.R. Jensen, *Prog. Mater. Sci.* **58**, 30 (2013).
9. M.Y. Song, S.H. Lee, Y.J. Kwak, Korean J. met. Mater. 59, 709 (2021).
10. B.C. Yeo, Korean J. met. Mater. 60, 537 (2022).
11. D.Y. Kim, S.-H. Park, Korean J. met. Mater. 60, 237 (2021).
12. J.J. Reilly and R.H. Wiswall Jr, *Inorg. Chem.* **7**, 2254 (1968).
13. M.Y. Song, H.R. Park, *J. Alloys. Compd.* **270**, 164 (1998).
14. J.F. Stampfer, C.E. Holley Jr. J.F. Suttle, *J. Amer. Chem. Soc.* **82**, 3504 (1960).
15. Lithium borohydride. https://en.wikipedia.org/wiki/Lithium_borohydride
16. A. Züttel, S. Rentsch, P. Fischer, P. Wenger, P, Sudan. Ph. Mauron, Emmenegger Ch. *J. Alloy Compd.* **356–357**, 515 (2003).
17. Z. Ding, S. Li, Y. Zhou, Z. Chen, W. Yang, W. Ma, L. Shaw, *Nano Mater. Sci.* **2**, 109 (2020).
18. J.J. Vajo, S.L. Skeith, F. Mertens, *J. Phys. Chem. B* **109**, 3719 (2005).
19. J.J. Vajo, G.L. Olson, *Scr. Matter* **56**, 829 (2007).
20. W.X. Zhang, X. Zhang, Z.G. Huang, H.W. Li, M.X. Gao, H.G. Pan, Y.F. Liu. *Adv. Energy Sustainability Res.***2**, 2100073 (2021).
21. F. Karimi, S. Börries, P.K. Pranzas, O. Metz, A. Hoell, G. Gizer, J.A. Puszkiel, M.V.C. Riglos, C. Pistidda, M. Dornheim, T. Klassen. *Adv. Eng. Mater.* **23**, 2100294 (2021).
22. Z. Ding, Y. Lu, L. Li, L. Shaw, *Energy Storage Mater.* **20**, 24 (2019).
23. Z. Ding, L. Shaw, *ACS Sustainable Chem. Eng.* **7**, 15064 (2019).
24. Z. Ding, H. Li, L. Shaw, *Chem. Eng. J.* **385**, 123856 (2020).
25. H.R. Park. M.Y. Song, *Korean J. Met. Mater.* **50**, 955 (2012).
26. M.Y. Song, S.N. Kwon, Y.J. Kwak, H.R. Park, *Mater. Res. Bull.* **48**, 74 (2013).
27. M.Y. Song, Y.J. Kwak, H.S. Shin, S.H. Lee, B.-G. Kim, *Int. J. Hydrogen Energy*, **38**, 1910 (2013).
28. M.Y. Song, Y.J. Kwak, S.H. Lee, H.R. Park, *Mater. Res. Bull.***48**, 2476 (2013).
29. D.M. Liu, Q.J. Tan, C. Gao, T. Sun, Y.T. Li, *Int. J. Hydrogen Energy*, **40**, 6600 (2015).
30. J. J. Vajo, W. Li, P. Liu, *Chem. Commun.* **46**, 6687 (2010).

31. N. Bergemann, C. Pistidda, M. Uptmoor, C. Milanese, A. Santoru, T. Emmler, J. Puszkiel, M. Dornheim, T. Klassen, *J. Energy Chem.* **34**, 240 (2019).
32. M.Y. Song, D.S. Ahn, I.H. Kwon, H.J. Ahn, *Met. Mater. Int.* **5**, 485 (1999).